山西大学学报(自然科学版)48(3):578—588,2025
Journal of Shanxi University(Nat. Sci. Ed.)

DOI:10.13451/j.sxu.ns.2024167

B、N和F共掺杂的新型碳点对硝唑类抗生素的检测

贾燕春[1,2],胡军辉[3],宋胜梅[1],双少敏[3],董川[1*]
(1.山西大学 环境科学研究所,山西 太原 030006;
2.山西大学 电力与建筑学院,山西 太原 030006;
3.山西大学 化学化工学院,山西 太原 030006)

摘 要:以氟硼酸钠、柠檬酸、乙胺和乙腈为前驱体,通过一步溶剂热法制备了硼、氮、氟共掺杂的蓝色荧光碳点(Blue Fluorescent Carbon Dots, BNF-CDs),分别利用透射电子显微镜、傅里叶变换红外光谱、X射线光电子能谱、紫外可见吸收和荧光光谱等对合成的BNF-CDs进行了结构、形貌及光学性能表征。结果表明,BNF-CDs具有稳定优异的光学性能,荧光量子产率高达65.9%。基于内滤作用,硝唑类抗生素可有效猝灭BNF-CDs的荧光,为甲硝唑类抗生素(Metronidazole, MTR)、奥硝唑类抗生素(Ornidazole, ORN)和替硝唑类抗生素(Tinidazole, TIN)的检测提供了一种新的荧光检测方法,并建立了相应的硝基咪唑类抗生素的检测曲线,线性范围分别为6 ~250 μmol/L、3.6 ~189 μmol/L和3.6 ~295 μmol/L,检出限分别为16 nmol/L、35 nmol/L、71 nmol/L。此外,对实际样品中MTR、ORN和TIN的测定也取得了满意的回收率(96.4%~105.8%),表明了该方法潜在的应用前景。

关键词:硝唑类抗生素;碳点;内滤效应;多功能检测
中图分类号:O657.3 **文献标志码**:A **文章编号**:0253-2395(2025)03-0578-11

A Novel Multifunctional Probe Based on Carbon Dots Co-doped B, N and F for Detection of Nitroimidazole Antibiotics

JIA Yanchun[1,2], HU Junhui[3], SONG Shengmei[1], SHUANG Shaomin[3], DONG Chuan[1*]
(1. *Institute of Environmental Science, Shanxi University, Taiyuan* 030006*, China;*
2. *School of Electric Power, Civil Engineering and Architecture, Shanxi University, Taiyuan* 030006*, China;*
3. *School of Chemistry and Chemical Engineering, Shanxi University, Taiyuan* 030006*, China*)

Abstract: Blue fluorescent carbon dots (BNF-CDs) co-doped with boron, nitrogen and fluorine were prepared by a one-step solvothermal method using sodium fluoroborate, citric acid, ethylamine and acetonitrile as precursors. Herein, the structure, morphology and optical properties of BNF-CDs were characterized by transmission electron microscopy, Fourier transform infrared spectrometer, X-ray photoelectron spectroscopy, UV-Vis absorption and fluorescence spectroscopy, respectively. The results illustrated that the BNF-CDs have stable and excellent optical properties with a high fluorescence quantum yield of 65.9%. Based on the internal filtration effect between BNF-CDs and nitroimidazole antibiotics, the fluorescence of BNF-CDs can be effectively quenched. This phenomenon provides a novel fluorescence method for the determination of metronidazole (MTR), ornidazole (ORN) and tinidazole (TIN), and the corresponding detection curves for these nitroimidazole antibiotics were established, with linear ranges of 6-250 μmol/L for MTR, 3.6-189 μmol/L for ORN and 3.6-295 μmol/L for TIN. The detection limits were found to be 16 nmol/L,

收稿日期:2024-07-22;**接受日期**:2024-11-19
基金项目:国家自然科学基金(22274090);山西省经方扶阳重点实验室(202104010910011);山西省基础研究项目(202203021221026);山西省专利转化项目(202306012)
作者简介:贾燕春(1974—),女,山西大同人,博士,讲师,研究方向为碳纳米材料。E-mail:jiayanchun@sxu.edu.cn
* **通信作者**:董川(DONG Chuan),E-mail:dc@sxu.edu.cn
引文格式:贾燕春,胡军辉,宋胜梅,等.B、N和F共掺杂的新型碳点对硝唑类抗生素的检测[J].山西大学学报(自然科学版),2025,48(3):578-588. DOI:10.13451/j.sxu.ns.2024167.

35 nmol/L and 71 nmol/L, respectively. In addition, satisfactory recovery rates (rangihg from 96.4% to 105.8%) have been achieved for determination of MTR, ORN and TIN in actual samples,which indicates its potential application in the future.
Key words: nitroimidazole antibiotics; carbon dots; internal filtration effect; multifunctional detection

1 Introduction

Nitroimidazole drugs, a class of synthetic organic compounds with a 5-nitroimidazole ring structure, are widely used as one of the antibiotics for the treatment of bacterial infection caused by human and animal protozoa and anaerobic bacteria. As early as 1978, the World Health Organization (WHO) listed metronidazole as the first choice of antibiotics against anaerobic infections. After over four decades of research, nitroimidazole antibiotics have been consistently developed and extensively utilized in various clinical medical fields, including anti-tuberculosis, antibacterial and antiviral treatments, as well as anti-inflammatory and antitumor applications[1-2]. In addition, nitroimidazole antibiotics are applied as additives to animal feed for preventing infection and cosmetics for eliminating inflammation and sterilization[3-5]. The high water solubility and low biodegradability of nitroimidazole antibiotics result in the frequent detection of nitroimidazole residues in various environments, including surface soil, municipal sewage, pharmaceutical waste, aquaculture and livestock effluents, as well as in food products such as eggs, milk, and other animal-derived items[5-6].

Nevertheless, the abuse of nitroimidazoles not only brings great risks to the ecological environment, but also directly endangers the biological safety. Once these drugs and their metabolites are delivered and enriched into the human body through the food chain, they can lead to serious symptoms such as neurotoxicity, anaphylactic shock, hepatotoxicity, even mutagenicity and carcinogenesis besides dizziness, nausea, insomnia and other symptoms[6-9]. Consequently, certain countries and regions, including China and the European Union, have implemented explicit bans on the use of such substances in food products derived from animals[6,10]. As a result, it is of great significance to monitor the contents of these drugs in animal tissues, excreta and feed, and the residues of nitroimidazole in organisms or environment[11-12].

At present, the analytical techniques for the determination of nitroimidazole residues mainly include gas chromatography[13], gas chromatography-mass spectrometry or tandem mass spectrometry[14], liquid chromatography[15], liquid chromatography tandem mass spectrometry[11], thin layer chromatography[16], enzyme-linked immunosorbent assay[3], capillary electrophoresis[17], and electrochemical analysis methods[18]. Although these methods exhibit the characteristics of high accuracy, sensitivity and selectivity, there are some problems such as cumbersome sample preparation, expensive instruments, and high detection costs, which limit their further applications. Therefore, the development of a nitroimidazole detection method with higher sensitivity, better selectivity, simpler operation and lower cost has become an important research topic in the field of environmental and food analysis.

Fluorescence analysis method has attracted much attention because of its cheap instrument, simple operation and high sensitivity and accuracy. Carbon dots (CDs), a novel fluorescent carbon material, has being paid more attention in recent years owing to their excellent performance and broad application prospects. Compared with traditional quantum dots, they not only exhibit stable and excellent optical properties, but also have favourable biocompatibility and environmental friendliness. These advantages give them potential applications in detecting[19-22], bioimaging[23-24], drug delivery[24-25], photocatalysis[26-27], optoelectronic devices[28-29], anti-counterfeiting[30], and so on. In terms of detection applications, many studies on CDs have focused on using CDs as

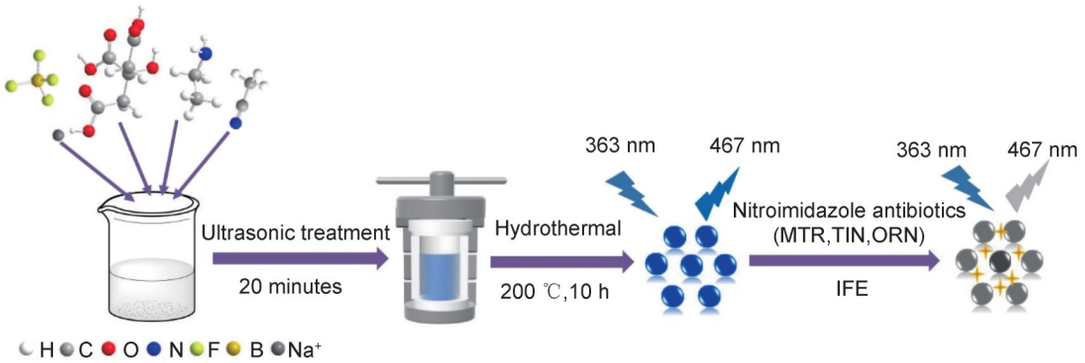

Scheme 1 Illustration for the synthetic procedure of the BNF-CDs using the hydrothermal method and the fluorescent sensing method for detection of nitroimidazole antibiotics (MTR, TIN, ORN)

a fluorescent probe to detect different targets, such as metal ions, inorganic anions, pH, temperature and organic pollutants based on the mechanism of fluorescence quenching and recovery[19-22]. Therefore, it is a good choice to design a fluorescence probe based on the CDs for realizing the sensitive detection of nitroimidazole antibiotics.

In this paper, blue fluorescent CDs (BNF-CDs) co-doped with boron, fluorine and nitrogen were prepared by one-step solvothermal method using sodium fluoroborate, citric acid, ethylamine and acetonitrile as precursors. As depicted as scheme 1, the fluorescence of the BNF-CDs can be effectively quenched by nitroimidazole antibiotics. The detection method of nitroimidazole was constructed based on the internal filtration effect (IFE) using metronidazole (MTR), ornidazole (ORN) and Tinidazole (TIN) as models. Compared with other detection methods, the method has the advantages of simple operation, good selectivity, wide detection ranges (the linear ranges of MTR, ORN and TIN are 6−250 μmol/L, 3.6−189 μmol/L and 3.6−295 μmol/L, respectively), and high sensitivity (the detection limits of MTR, ORN and TIN are 16 nmol/L, 35 nmol/L and 71 nmol/L, respectively).

2 Experimental Section

2.1 Chemicals

Sodium fluoroborate, citric acid, ethylamine, acetonitrile, various metal chloride salts, and various antibiotics MTR, ORN, TIN, cefradine (CED), cefotaxime (CTX), penicillin (PEN), amoxicillin (AMX), ampicillin (AMP), streptomycin (STR), gentamicin (GEN), kanamycin (KAN), erythromycin (ERY), azithromycin (AZM), clarithromycin (CLR), oxytetracycline (CTE), tetracycline(TCY), Lincomycin (LIN), clindamycin (CLI), sulfadiazine (SDI), sulfamethoxazole (SMZ), Trimethoprim (TMP), ciprofloxacin (CIP), norfloxacin(NOR), levofloxacin (LVX), chloramphenicol (CHL), thiamphenicol (THI), vancomycin (VAN)) were all analytical grade and obtained from Aladdin Reagent Co., Ltd. The dialysis membrane (MWCO = 500−1 000 Da) was acquired from Spectrum Laboratories (Rancho Dominguez, CA, USA). The experimental water was ultrapure water (≥ 18.25 MΩ·cm).

2.2 Preparation of BNF-CDs

The synthesis process is depicted in Scheme 1. 2.5 g of sodium fluoroborate, 1.0 g of citric acid, 5 mL of ethylamine and 25 mL of acetonitrile were transferred into a 100 mL of beaker. After stirring and ultrasonic treatment for 20 minutes, the homogeneous dispersed solution was poured into a polytetrafluoroethylene reactor and heated for 10 h at 200 ℃. Next, when cooling to room temperature, the solution in the reactor was poured out and filtered to remove the filter residue. And then, the filtrate was dialyzed by dialysis tube (M 500 −1 000 DA) for 5 h and recharged the water every one hour. After that, the brown solid powder BNF-CDs was obtained by freeze-drying and stored for following experiments.

2.3 Characterization of BNF-CDs

The morphology and lattice of BNF-CDs were observed by using a JEOLJEM-2100 transmission electron microscopy (TEM) (Tokyo, Japan). The composition and relative content of BNF-CDs were determined by element analyzer and inductively coupled plasma mass spectrometer (ICP-Mass). The existing state of elements in BNF-CDs was characterized by X-ray photoelectron spectroscopy (XPS) and Fourier transform infrared spectrometer (FTIR). The doping forms of B, N and F and surface functional groups of BNF-CDs were determined by FT-IR and XPS. The optical properties of BNF-CDs were characterized by UV and VIS spectrophotometer. The content of MTR, ORN and TIN was detected by fluorescence spectrometer.

2.4 Fluorescence quantum yield of BNF-CDs

The relative fluorescence quantum yield of BNF-CDs was calculated by the following formula.

$$\Phi_S = \Phi_R(I_S/A_S)\ (A_R/I_R)(\eta_S^2/\eta_R^2)$$

Among them, Rhodamine B was used as the reference solution. Φ, I, A and η represent fluorescence quantum yield, integral fluorescence intensity (fluorescence integral area is 380 nm−600 nm), absorbance intensity and refractive index of solvent, respectively. Subscripts S and R represent BNF-CDs and Rhodamine B reference solution, respectively. The excitation wavelength is 363 nm and the emission wavelength is 467 nm. To prevent the effect of solution re-absorption effectively, the absorbance intensity was kept less than 0.1.

2.5 Selectivity of BNF-CDs to nitroimidazole antibiotics

20 μL of various ions (0.1 mol/L) and antibiotic drugs (0.01 mol/L) were added to 2.5 mL of BNF-CDs solution (24 μg/mL). The fluorescence intensities were recorded before and after the addition of these substances at excitation and emission wavelengths of 363 nm and 467 nm, respectively.

2.6 Detection of nitroimidazole antibiotics

For the detection of nitroimidazole antibiotics, MTR, ORN, and TIN were applied as the representatives of nitroimidazole antibiotics. Appropriate amounts of samples were added to 2 mL of BNF-CDs solution sequentially, and the fluorescence intensities of the solution were recorded at the excitation and emission wavelengths of 363 nm and 467 nm, respectively.

3 Results and Discussion

3.1 Structural characterization of BNF-CDs

The elemental analysis results are presented in Table S1, showing that the BNF-CDs consisted of C 7.99, H 1.26, O 9.85, N 1.38, B 2.01, and F (calculated) 77.51%, respectively. And the empirical formula of a BNF-CD is $C_{13}H_{13}O_6NB_2F_{41}$ (Table S2).

The size and morphology of BNF-CDs are exhibited in Fig. 1, which indicates that BNF-CDs are uniform and mono-disperse spherical shape. And the average particle size is 3.97 nm with a narrow particle size distribution range of 1.75−7.00 nm (middle illustration in Fig. 1). Furthermore, the crystal structure of BNF-CDs is observed obviously, and the lattice spacing is about 0.21 nm consistent with the (100) surface of graphite carbon [31-32] (upper right illustration in Fig. 1) of BNF-CDs.

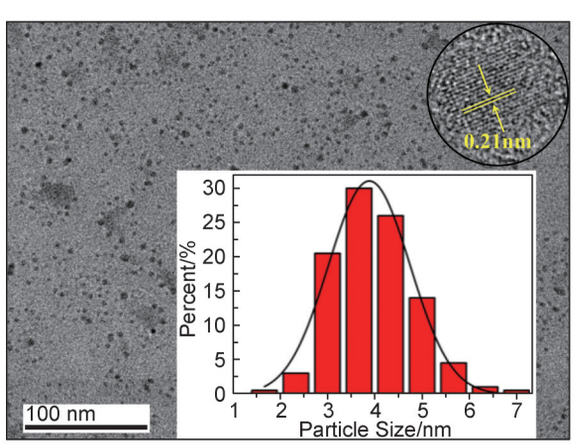

Fig. 1 The image of TEM (inset: the size distribution)

The composition and surface functional groups of the BNF-CDs were investigated by FTIR and XPS. As shown in Fig. 2(a), there is a broad characteristic absorption peak from 3 195 to 3 300 cm^{-1}, which is attributed to the stretching vibration of O—H and N—H[32-33]. The sharp absorption peaks at 3 100 cm^{-1},

2 979 cm^{-1} and 1 690 cm^{-1} are corresponded to ═C—H, C—H and C═O bands, respectively[33]. The peak at 1 407 cm^{-1} manifests the existence of aromatic C—N stretching vibration, and the absorption peaks at 1 050−1 119 cm^{-1} is ascribed to C—F/C—O/C—B bonds[34-38].

The surface elemental contents and states for the prepared BNF-CDs were investigated by XPS (Fig. 2(b)). The full XPS spectra contain five characteristic peaks located at 285.0, 400.0, 195.0, 532.0 and 687.0 eV, corresponding to C1s, N1s, B1s, O1s and F1s, respectively. High resolution C1s spectrum is attributed to C—B/C—C/C—N (284.7 eV), C—O (285.3 eV), C═O (286.4 eV) and C—F (288.4 eV), respectively (Fig. 2(c)) [34-35,39]. The deconvoluted high-resolution N1s spectrum is divided into two peaks at 400.0 and 401.6 eV, indicating the existence of N—C and N—H (Fig. 2(d))[36]. B1s spectrum is assigned to B—C (193.0 eV) and B—O (195.5 eV), respectively (Fig. S1(a))[34-36]. O1s spectrum exhibits two peaks at 531.9 and 533.3 eV, implying the existence of C—O and C═O, respectively (Fig. S1(b)) [37]. Moreover, the F1s spectrum includes a single peak at 687.3 eV corresponding to C—F (Fig. S1(c))[31,34]. Based on the above results, B, N and F had been successfully doped into the CDs. These results are consisted with the results of element analyser and ICP-Mass, and the surface of BNF-CDs features rich heterocycles with conjugated structures and hydrophilic groups, which facilitate interactions between the BNF-CDs and nitroimidazole antibiotics.

3.2 Optical properties of BNF-CDs

To investigated the optical property of the BNF-CDs, the UV-Vis absorption and fluorescence spectra were performed. As seen from Fig. 3(a), the UV absorption spectrum of BNF-CDS has three absorption peaks at 235 nm, 365 nm and 460 nm, re-

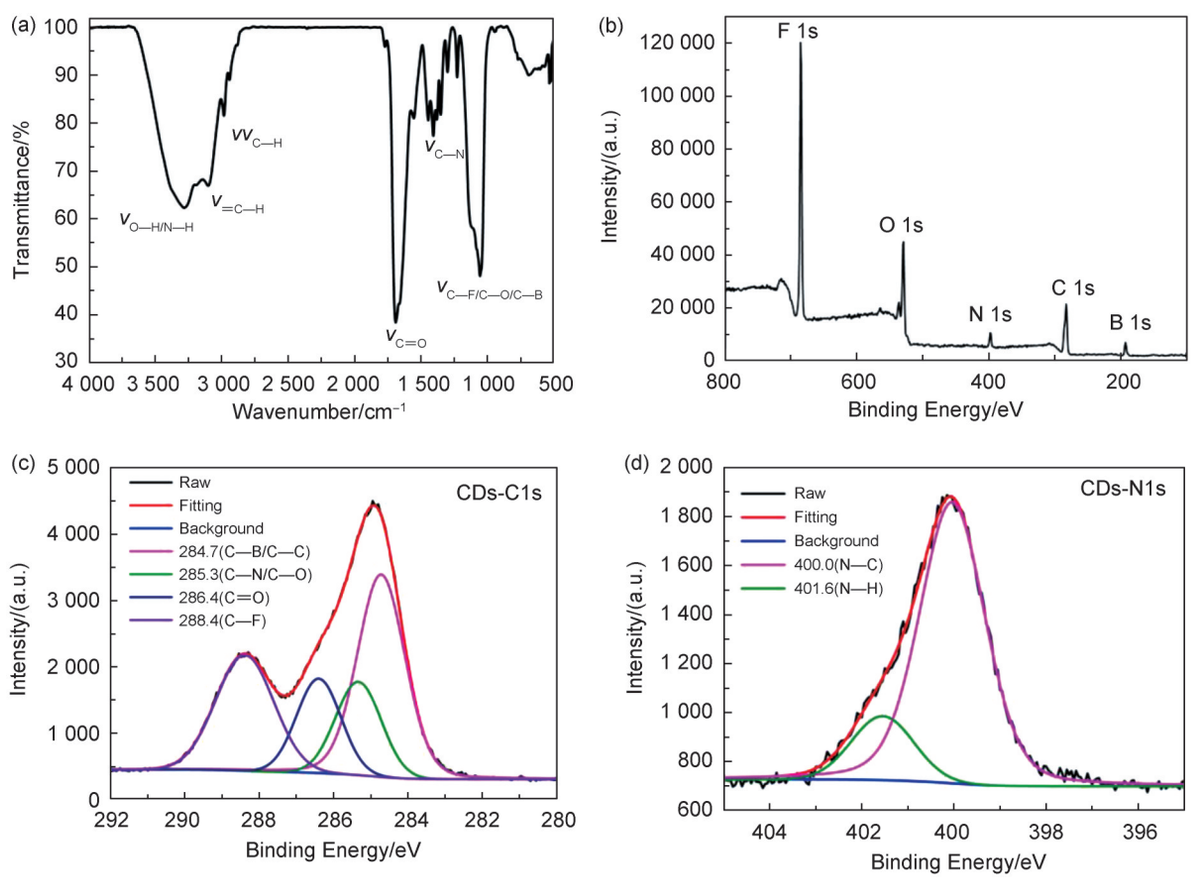

Fig. 2 The composition and surface functional groups of the BNF-CDs

(a) FTIR, (b) XPS spectrum, (c) C1s, and (d) N1s High resolution XPS spectra of BNF-CDs

spectively. The absorption peak at 235 nm may be ascribed to the π－π* transition of C═C bond[31,40]. There is a wide absorption band at 300−400 nm, which is due to the π－π* transition of C═C bond, n-π* transition of C═O bond and surface defect states caused by the nitrogen-doped conjugate structure[31]. The absorption peak at 460 nm may contribute to various functional groups on the surface of BNF-CDs[41]. The fluorescence excitation and emission spectra of the BNF-CDs aqueous solution in Fig. 3(a) indicates that there is a maximum emission peak at 467 nm under 363 nm excitation. In addition, as exhibited in Fig. 3(b), when the excitation wavelength increases from 320 nm to 400 nm, the emission of BNF-CDs only has a slight red shift, showing its non-excitation dependent characteristics. Three-dimensional (3D) fluorescence of BNF-CDs aqueous solution were also performed (Fig. 3(c)), and BNF-CDs exhibit the strongest excitation and emission peaks at 363 nm and 467 nm, respectively, which may be caused by narrow size distribution and homogeneous species. Furthermore, the quantum yield of BNF-CDs was also measured using rhodamine B as reference, which is up to 65.9% (Fig. S2).

The optical stability of BNF-CDs was examined and its results demonstrated in Fig. 4. After 180 minutes of continuous exposure Xenon lamp, the fluorescence intensities of BNF-CDs only changed slightly (Fig. 4(a)), indicating its excellent photobleaching resistance. Moreover, the fluorescence intensities of BNF-CDs were relatively strong and changed little in the range of pH 4.00−10.00 (Fig. 4 (b)), implying that BNF-CDs can be applied in a wide pH range. Furthermore, the impact of ionic strength on the fluorescence of BNF-CDs was also discussed, and it proved that high ionic strength had little effect on the fluorescence property of BNF-CDs (Fig. 4(c)). As mentioned above, the BNF-CDs has good optical stability, and the external environmental factors such as the illumination, pH and the high ion strength have negligible influence on the BNF-CDs optical properties. Therefore, the prepared BNF-CDs have a wide range of applications.

3.3 Detection of nitroimidazole antibiotics by BNF-CDs

Based on the previous analysis results, there are many active functional group structures on the surface of BNF-CDs, and it would be applied as a potential fluorescence probe. A certain concentration of 28 antibiotics, 19 cations and 14 anions were added into the BNF-CDs aqueous solution with a concentration of 0.24 mg/mL, and the results were displayed in Fig. 5. It can be quenched by three nitroimidazole antibiotics. Meanwhile, other antibiotics and other common ions have a low or a negligible effect on fluorescence of BNF-CDs. Moreover, the BNF-CDs shown in Fig. S3 detected the anti-interference ability of the three nitroimidazole antibiotics, showing that there was no significant change in the degree of fluorescence quenching when other antibiotics coexisted with MTR, ORN, and TIN, re-

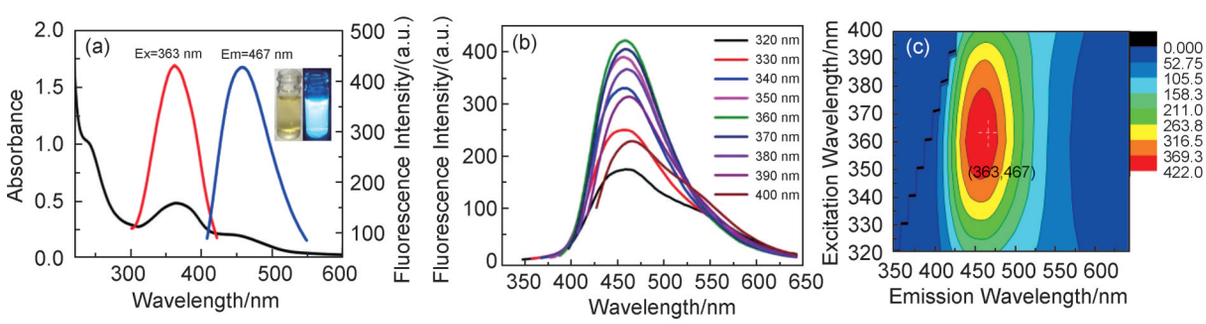

Fig. 3 Optical characterizations of BNF-CDs

(a) UV-Vis absorption image of BNF-CDs and its excitation/emission spectra; (b) Fluorescence emission spectra of BNF-CDs under different excitations wavelengths (320−400 nm) in 10 nm increments; (c) 3D fluorescence plots of aqueous BNF-CDs

spectively. In addition, reaction time between the BNF-CDs and the three antibiotics was also studied (Fig. S4), they reacted rapidly and no more than 15 s. All these indicate that BNF-CDs can specifically and quickly identify nitroimidazole antibiotics from relatively complex environments.

Thereafter, the sensitivity of BNF-CDs to nitroimidazole drugs was evaluated using MTR, ORN and TIN as representatives. As shown in Fig. 6 and Fig. S5, the fluorescence intensities of BNF-CDs gradually decrease with the continuous addition of the three kinds of nitroimidazoles. Additionally, the ratio of fluorescence intensities of (F_0/F) exhibits a significant linear correlation with the concentration of antibiotics within a certain range. The linear ranges of MTR, ORN and TIN are 6−250 μmol/L (n=3), 3.6−189 μmol/L (n=3) and 3.6−295 μmol/L (n=3), and the detection limits (LODs) are 16 nmol/L (2.74 ng/mL), 35 nmol/L (7.69 ng/mL) and 71 nmol/L (17.56 ng/mL), respectively. Therefore, BNF-CDs demonstrate a wide detection range and a low LOD for nitroimidazole antibiotics. This indicates that BNF-CDs have promising potential for application in detecting nitroimidazole antibiotics in complex environments. Furthermore, a comparison of the proposed work with other reported literature on the determination of nitroimidazoles is revealed in Table S3, highlighting the clear advantages of the established analytical method.

3.4 The Interaction mechanism of BNF-CDs and nitroimidazoles antibiotics

To further explore the fluorescence quenching mechanism of BNF-CDs by nitroimidazole antibiotics, FL, UV-vis absorption, and fluorescence lifetime were studied. As shown in Fig. 7(a), the excitation spectrum of BNF-CDs partially overlaps with the absorption spectra of MTR, ORN and TIN. This overlap causes the nitroimidazoles to preemptively

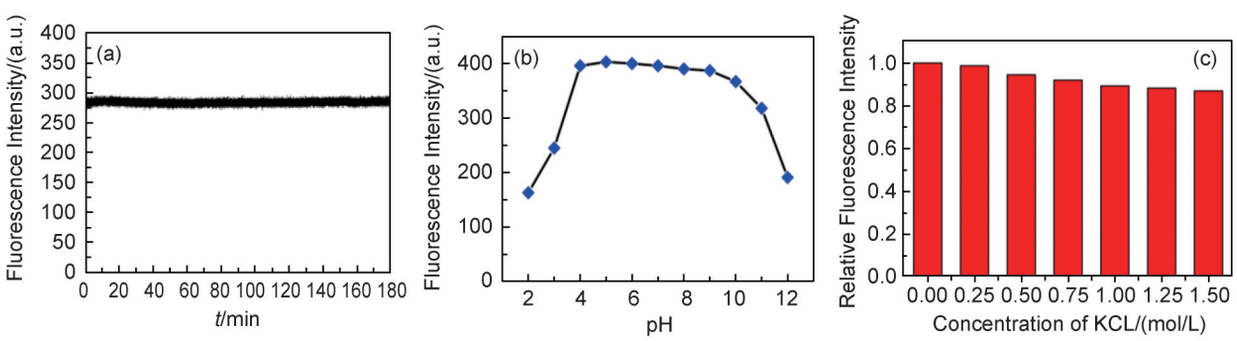

Fig. 4 Fluorescence intensity of BNF-CDs under different
(a) illumination time, (b) pH (2. 00−12. 00), and (c) ionic strength

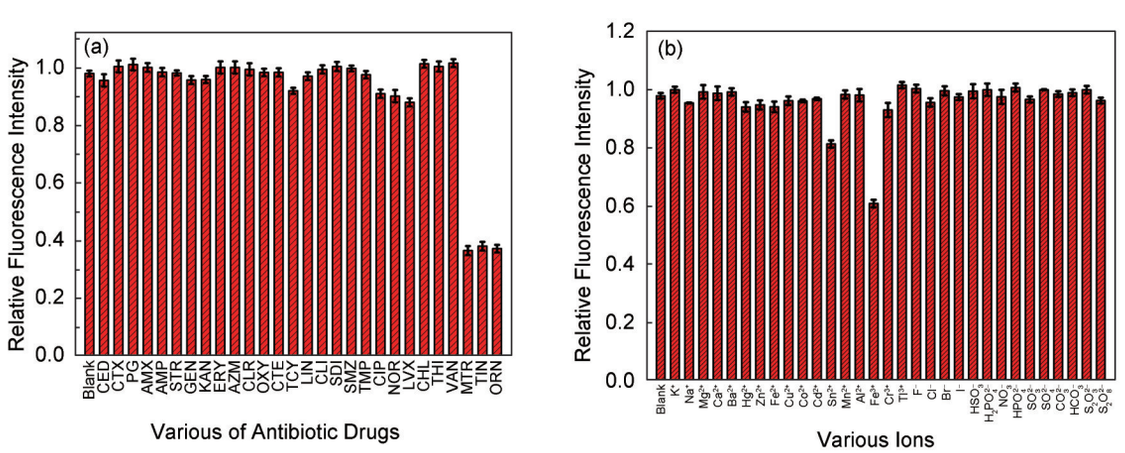

Fig. 5 Relative fluorescence intensity of BNF-CDs after adding different
(a) antibiotics and (b) metal ions and anions

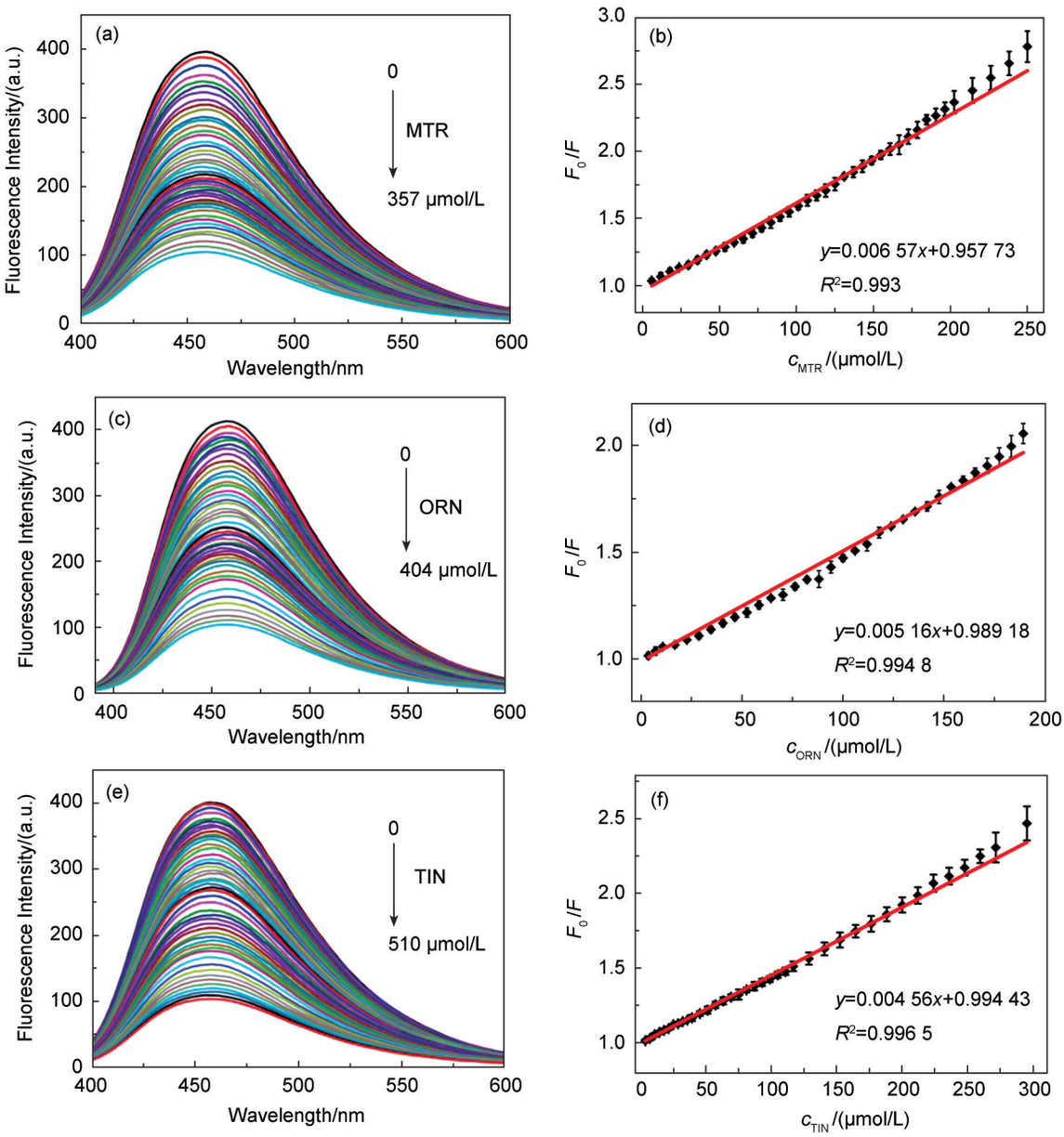

Fig. 6 The fluorescence quenching curve of BNF-CDs by (a) MTR, (c) ORN, and (e) TIN, and the linear fitting curves between the concentrations of (b) MTR, (d) ORN, and (f) TIN with F_0/F

absorb the energy from the excited BNF-CDs, which in turn quenches the fluorescence of BNF-CDs. In addition, from Fig. 7(b), the fluorescence lifetime of BNF-CDs was hardly variable after MTR, ORN and TIN introduction. Therefore, internal filter effect (IFE) or static quenching (SQ) may be responsible for the fluorescence change of BFD-CDs before and after the addition of nitroimidazoles. However, as can been seen from Fig. S6 and Fig. 6, after the addition of MTR, ORN and TIN, the peaks of UV absorption and fluorescence emission of BNF-CDs had no shift, inferring that no new fluorescent substances were generated in the mixture of BNF-CDs/nitroimidazoles[28], suggesting that static quenching mechanism could be ruled out. Therefore, the continuous addition of nitroimidazole further promotes the fluorescence quenching, which based on the IFE between BNF-CDS and nitroimidazoles.

3.5 Detection in real samples

The established method was applied for the detection of three antibiotics in milk, and none of them was detected. Then the spiked addition recov-

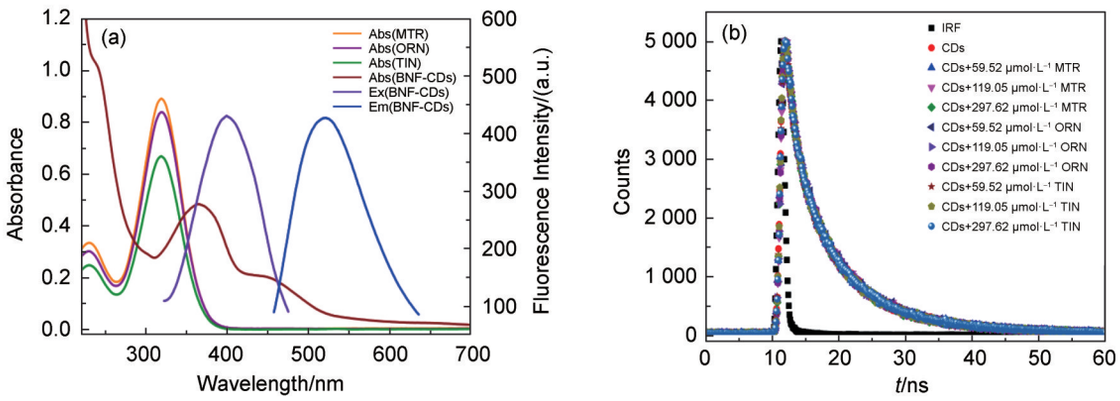

Fig. 7 Illustration of the fluorescence quenching mechanism of BNF-CDs

(a) UV-Vis absorption spectra of BNF-CDs, MTR, ORN and TIN and excitation/emission spectra of BNF-CDs; (b) Fluorescence emission decay curves of BNF-CDs, BNF-CDs/MTR, BNF-CDs/ORN and BNF-CDs/TIN (IRF is the instrumental response function curve)

ery experiments were carried out in the linear range, and the results were shown in Table S4. It can be seen from the Table S4 that the standard addition recovery rate is within (100±10)%, and the standard deviation is less than 5%, so the established analytical method is practical.

4 Conclusion

Bright blue fluorescent BNF-CDs were synthesized using a one-step hydrothermal method with sodium fluoroborate, citric acid, ethylamine, and acetonitrile as precursors. The synthesized BNF-CDs exhibit a high quantum yield and excellent optical stability under prolonged illumination, across a pH range of 4.00 to 10.00, and in high ion concentrations. Furthermore, the fluorescence of BNF-CDs can be quenched by nitroimidazole antibiotics. Consequently, based on the IFE, a fluorescence method for detecting nitroimidazole antibiotics using BNF-CDs was developed, demonstrating significant selectivity and high sensitivity. Additionally, this method was applied in standard addition recovery experiments, achieving satisfactory results. This indicates that it offers a low-cost and convenient approach for determining nitroimidazole residues in complex environmental samples.

Reference:

[1] ANG C W, JARRAD A M, COOPER M A, *et al*. Nitroimidazoles: Molecular Fireworks That Combat a Broad Spectrum of Infectious Diseases[J]. *J Med Chem*, 2017, **60** (18): 7636−7657. DOI: 10.1021/acs.jmedchem.7b00143.

[2] ZHANG J Y, BA Y Y, WANG S, *et al*. Nitroimidazole-containing Compounds and Their Antibacterial and Antitubercular Activities[J]. *Eur J Med Chem*, 2019, **179**: 376−388. DOI: 10.1016/j.ejmech.2019.06.068.

[3] ZHANG C, PAN J, SHUAI R, *et al*. Research on Enzyme Linked Immunosorbent Assay for Multi-residues of Nitroimidazoles in Foods of Animal Origin[J]. *J Nucl Agri Sci*, 2016, **30**(2): 323−331. DOI: 10.11869/j.issn.100-8551.2016.02.0323.

[4] ZHANG L T, HUANG S, YANG X, *et al*. Determination of Six Kinds of Antibiotics and Metronidazole in Anti-acne Cosmetics by High Performance Liquid Chromatography[J]. *Chin J Anal Lab*, 2015, **34**(12): 1403−1407. DOI: 10.13595/j.cnki.issn1000-0720.2015.0307.

[5] PENG Y G, ZHANG Y X, HUANG H L, *et al*. Flexibility Induced High-performance MOF-based Adsorbent for Nitroimidazole Antibiotics Capture[J]. *Chem Eng J*, 2018, **333**: 678−685. DOI: 10.1016/j.cej.2017.09.138.

[6] ZELENY R, SCHIMMEL H, ULBERTH F, *et al*. Development of a Certified Reference Material for the Content of Nitroimidazole Parent Drugs and Hydroxy Metabolites in Pork Meat[J]. *Anal Chim Acta*, 2009, **634**(2): 237−242. DOI: 10.1016/j.aca.2008.12.019.

[7] XU P, LUO X, CHENG R. Determination of 10 Kinds of Nitroimidazole Substances in Herbal Tea by Ultra Performance Liquid Chromatography-tandem Mass Spectrometry[J]. *J Food Saf Food Qual*, 2024, **15** (14): 84−92. DOI: 10.19812/j.cnki.jfsq11-5956/ts.20240422001.

[8] RAETHER W, HÄNEL H. Nitroheterocyclic Drugs with Broad Spectrum Activity[J]. *Parasitol Res*, 2003,

90Supp 1: S19−S39. DOI: 10.1007/s00436-002-0754-9.

[9] VOOGD C E. On the Mutagenicity of Nitroimidazoles [J]. *Mutat Res*, 1981, **86**(3): 243−277. DOI: 10.1016/0165-1110(81)90006-3.

[10] GB/T 31650−2019, National Food Safety Standard−Maximum Residue Limits for Veterinary Drugs in Foods[S].

[11] ZHANG W, FENG D, *et al*. Determination of Nitroimidazole Residues in Eggs Ultra Performance Liquid Chromatography-Tandem Mass Spectrometry [J]. *Chin J Anim Infec*, 2023, **7**: 1−10. DOI: 10.19958/j.cnki.cn31-2031/s.20230720.001.

[12] MAHUGO-SANTANA C, SOSA-FERRERA Z, TORRES-PADRÓN M E, *et al*. Analytical Methodologies for the Determination of Nitroimidazole Residues in Biological and Environmental Liquid Samples: a Review[J]. *Anal Chim Acta*, 2010, **665**(2): 113−122. DOI: 10.1016/j.aca.2010.03.022.

[13] LIU B, HUANG W, WANG J. Simultaneous Determination of Nitroimidazole by Gas Chromatography-Electron Capture Detector[J]. *J Anal Sci*, 2008, **24**(5): 586−588. DOI: 1006-6144(2008) 05-0586-03.

[14] DONG H, YING L, PING X, *et al*. Quantitative Determination of 4 Nitroimidazoles in Acne Cosmetics by Gas Chromatography-Mass Spectrometry[J]. *J Ins Anal*, 2015, **34**(8): 911−916. DOI: 10.3969/j. issn. 1004-4957. 2015. 08. 008

[15] WANG Y, ZHENG C, FENG H, *et al*. Simultaneous Determination of Nitroimidazoles Multi-residues in Tilapia Muscle by High Performance Liquid Chromatography[J]. *Food Sci*, 2011, **32**(20): 197−199. DOI: 10.1090/S0002-9939-2011-10775-5.

[16] GATTAVECCHIA E, TONELLI D. Thin-layer Chromatography of some 5-Nitroimidazoles of Pharmaceutical Interest[J]. *J Chromatogr A*, 1980, **193**(2): 340−342. DOI: 10.1016/s0021-9673(00)81508-3.

[17] YANG X P, CHENG X M, LIN Y Y, *et al*. Determination of Three Nitroimidazoles in Rabbit Plasma by Two-step Stacking in Capillary Zone Electrophoresis Featuring Sweeping and Micelle to Solvent Stacking[J]. *J Chromatogr A*, 2014, **1325**: 227−233. DOI: 10.1016/j.chroma.2013.11.053.

[18] WANG H X, BO X J, ZHOU M, *et al*. DUT-67 and Tubular Polypyrrole Formed a Cross-linked Network for Electrochemical Detection of Nitrofurazone and Ornidazole[J]. *Anal Chim Acta*, 2020, **1109**: 1−8. DOI: 10.1016/j.aca.2020.03.002.

[19] LI W K, FENG J T, MA Z Q. Nitrogen, Sulfur, Boron and Flavonoid Moiety Co-incorporated Carbon Dots for Sensitive Fluorescence Detection of Pesticides[J]. *Carbon*, 2020, **161**: 685−693. DOI: 10.1016/j.carbon.2020.01.098.

[20] ZHU J T, CHU H Y, SHEN J W, *et al*. Nitrogen and Fluorine Co-doped Green Fluorescence Carbon Dots as a Label-free Probe for Determination of Cytochrome *c* in Serum and Temperature Sensing[J]. *J Colloid Interface Sci*, 2021, **586**: 683−691. DOI: 10.1016/j.jcis.2020.10.138.

[21] WANG Y L, LAO S Y, DING W J, *et al*. A Novel Ratiometric Fluorescent Probe for Detection of Iron Ions and Zinc Ions Based on Dual-emission Carbon Dots[J]. *Sens Actuat B Chem*, 2019, **284**: 186−192. DOI: 10.1016/j.snb.2018.12.139.

[22] JIA Y C, CHENG Z, WANG G H, *et al*. Nitrogen Doped Biomass Derived Carbon Dots as a Fluorescence Dual-mode Sensing Platform for Detection of Tetracyclines in Biological and Food Samples[J]. *Food Chem*, 2023, **402**: 134245. DOI: 10.1016/j.foodchem.2022.134245.

[23] WANG H P, ZHANG L, GUO X Q, *et al*. Comparative Study of Cl, N-Cdots and N-Cdots and Application for Trinitrophenol and ClO^- Sensor and Cell-imaging[J]. *Anal Chim Acta*, 2019, **1091**: 76−87. DOI: 10.1016/j.aca.2019.09.019.

[24] SHU Y, LU J, MAO Q X, *et al*. Ionic Liquid Mediated Organophilic Carbon Dots for Drug Delivery and Bioimaging[J]. *Carbon*, 2017, **114**: 324−333. DOI: 10.1016/j.carbon.2016.12.038.

[25] DEVI P, SAINI S, KIM K H. The Advanced Role of Carbon Quantum Dots in Nanomedical Applications[J]. *Biosens Bioelectron*, 2019, **141**: 111158. DOI: 10.1016/j.bios.2019.02.059.

[26] PEI Y F, SONG H Q, LIU Y, *et al*. Boron-nitrogen-doped Carbon Dots on Multi-walled Carbon Nanotubes for Efficient Electrocatalysis of Oxygen Reduction Reactions[J]. *J Colloid Interface Sci*, 2021, **600**: 865−871. DOI: 10.1016/j.jcis.2021.05.089.

[27] SHARMA S, DUTTA V, SINGH P, *et al*. Carbon Quantum Dot Supported Semiconductor Photocatalysts for Efficient Degradation of Organic Pollutants in Water: a Review[J]. *J Clean Prod*, 2019, **228**: 755−769. DOI: 10.1016/j.jclepro.2019.04.292.

[28] LI X M, RUI M C, SONG J Z, *et al*. Carbon and Graphene Quantum Dots for Optoelectronic and Energy Devices: a Review[J]. *Adv Funct Materials*, 2015, **25**(31): 4929−4947. DOI: 10.1002/adfm.201501250.

[29] GUAN Q W, SU R G, ZHANG M R, *et al*. Highly Fluorescent Dual-emission Red Carbon Dots and Their Ap-

plications in Optoelectronic Devices and Water Detection[J]. *New J Chem*, 2019, **43**(7): 3050−3058. DOI: 10.1039/C8NJ06074F.

[30] JIANG K, ZHANG L, LU J, *et al*. Triple-mode Emission of Carbon Dots: Applications for Advanced Anti-counterfeiting[J]. *Angew Chem Int Ed Engl*, 2016, **55**(25): 7231−7235. DOI: 10.1002/anie.201602445.

[31] LIU F, LI Z Y, LI Y, *et al*. Room-temperature Phosphorescent Fluorine-nitrogen Co-doped Carbon Dots: Information Encryption and Anti-counterfeiting[J]. *Carbon*, 2021, **181**: 9−15. DOI: 10.1016/j.carbon.2021.05.023.

[32] LU X H, WANG W, DONG Q, *et al*. A Multi-functional Probe to Discriminate Lys, Arg, His, Cys, Hcy and GSH from Common Amino Acids[J]. *Chem Commun*, 2015, **51**(8): 1498−1501. DOI: 10.1039/c4cc07757a.

[33] WU S S, LI W, SUN Y Q, *et al*. Synthesis of Dual-emissive Carbon Dots with a Unique Solvatochromism Phenomenon[J]. *J Colloid Interface Sci*, 2019, **555**: 607−614. DOI: 10.1016/j.jcis.2019.07.089.

[34] LONG P, FENG Y Y, CAO C, *et al*. Carbon Dots: Self-protective Room-temperature Phosphorescence of Fluorine and Nitrogen Codoped Carbon Dots[J]. *Adv Funct Materials*, 2018, **28**(37): 1870263. DOI: 10.1002/adfm.201870263.

[35] LEE J W, OLIVEIRA M T, JANG H B, *et al*. Hydrogen-bond Promoted Nucleophilic Fluorination: Concept, Mechanism and Applications in Positron Emission Tomography[J]. *Chem Soc Rev*, 2016, **45**(17): 4638−4650. DOI: 10.1039/c6cs00286b.

[36] DING H, YU S B, WEI J S, *et al*. Full-color Light-emitting Carbon Dots with a Surface-state-controlled Luminescence Mechanism[J]. *ACS Nano*, 2016, **10**(1): 484−491. DOI: 10.1021/acsnano.5b05406.

[37] LIU Y L, ZHOU Q X, YUAN Y Y, *et al*. Hydrothermal Synthesis of Fluorescent Carbon Dots from Sodium Citrate and Polyacrylamide and Their Highly Selective Detection of Lead and Pyrophosphate[J]. *Carbon*, 2017, **115**: 550−560. DOI: 10.1016/J.CARBON.2017.01.035.

[38] YU J, SONG N, ZHANG Y K, *et al*. Green Preparation of Carbon Dots by Jinhua Bergamot for Sensitive and Selective Fluorescent Detection of Hg^{2+} and Fe^{3+} [J]. *Sens Actuat B Chem*, 2015, **214**: 29−35. DOI: 10.1016/j.snb.2015.03.006.

[39] ZHANG H J, CAI C L, MA Z F, *et al*. N, F Dual-doped Carbon Embedded with Co&CoN Paragenetic Structure for Oxygen Electrocatalytic Reduction Reaction[J]. *Int J Hydrog Energy*, 2021, **46**(10): 7454−7463. DOI: 10.1016/j.ijhydene.2020.11.203.

[40] YU C H, QIN D M, JIANG X H, *et al*. Facile Synthesis of Bright Yellow Fluorescent Nitrogen-doped Carbon Quantum Dots and Their Applications to an Off-on Probe for Highly Sensitive Detection of Methimazole [J]. *Microchem J*, 2021, **168**: 106480. DOI: 10.1016/j.microc.2021.106480.

[41] DANG D K, SUNDARAM C, NGO Y L T, *et al*. Pyromellitic Acid-derived Highly Fluorescent N-doped Carbon Dots for the Sensitive and Selective Determination of 4-Nitrophenol[J]. *Dyes Pigm*, 2019, **165**: 327−334. DOI: 10.1016/j.dyepig.2019.02.029.